

VIRTUAL PASSIVITY-BASED DECENTRALIZED CONTROL OF MULTIPLE 3-WHEELED MOBILE ROBOTIC SYSTEMS VIA SYSTEM AUGMENTATION

J. H. SUH¹⁾ and K. S. LEE^{1)*}

¹⁾Department of Electrical Engineering, Dong-A University, Busan 604-714, Korea

(Received 18 May 2004; Revised 23 April 2005)

ABSTRACT—Passive velocity field control (PVFC) was previously developed for fully mechanical systems, in which the motion task was specified by behaviors in terms of a velocity field and the closed-loop was passive with respect to the supply rate given by the environment input. However, the PVFC was only applied to a single manipulator. The proposed control law was derived geometrically and the geometric and robustness properties of the closed-loop system were also analyzed. In this paper, we propose a virtual passivity-based algorithm to apply decentralized control to multiple 3-wheeled mobile robotic systems whose subsystems are under nonholonomic constraints and convey a common rigid object in a horizontal plain. Moreover, it is shown that multiple robot systems ensure stability and the velocities of augmented systems converge to a scaled multiple of each desired velocity field for cooperative mobile robot systems. Finally, the application of proposed virtual passivity-based decentralized algorithm via system augmentation is applied to trace a circle and the simulation results is presented in order to show effectiveness for the decentralized control algorithm proposed in this research.

KEY WORDS : Decentralized control, Passive velocity field control (PVFC), Augmented system, Minor loop compensation, Passivity, Wheeled mobile robot, Automated guided vehicle (AGV)

1. INTRODUCTION

The manipulation task of a mechanical system is traditionally specified by means of a desired time trajectory in the workspace. The control objective is to track this trajectory at every instant of time. Moreover, in the context of machining, the system has to interact closely with its physical environment. When the contour following task is represented by a velocity field on the configuration manifold of the system, the coordination aspect of the problem is made explicit. Therefore, the passive velocity field control (PVFC) scheme can then be applied to track the defined velocity field so that the desired contour is followed, and to ensure that the interaction of the closed-loop system with the physical environment is passive to enhance safety and stability (Li *et al.*, 1999 and 2001).

However, the PVFC algorithm applied to a single manipulator could not extend to multiple robotic systems. Especially, multiple robotic systems can execute various tasks which could not be done by a single manipulator such as the handling of a heavy object, for example,

transportation of port containers using cooperative AGV systems. Therefore, many control algorithms have been proposed for the coordinated motion control of multiple robot systems. That is, the typical algorithms for multiple robotic systems may be summarized as follows: i) centralized control algorithm; and ii) decentralized control algorithm. Moreover, various decentralized control algorithms have been proposed to overcome some problems of the centralized control algorithm in which each robot system is controlled by its own controller without explicit communication among cooperative systems.

In our previous research (Yamakita *et al.*, 1998), the decentralized implementation of PVFC including internal force control was proposed in a case where an object is rigidly grasped by multiple manipulators. In this paper, we propose a method to apply an original PVFC with some modification to cooperative mobile robotic systems which consist of two planar mobile robots which convey a common rigid object attached to mobile robots with passive rotational joints in a horizontal plain. Each mobile robot is a 3-wheeled mobile robot and is under nonholonomic constraints. The specifications of proposed controller are as follows:

*Corresponding author. e-mail: kslee@dau.ac.kr

- (1) The center of the object follows a desired velocity field without external disturbances;
- (2) The orientation of the object tracks a desired value specified in terms of the position of center of an object;
- (3) Linear motion of an object has properties of a system controlled by an original PVFC;
- (4) Internal force is controlled in a certain direction.

Moreover, it is shown that multiple robot systems ensure stability and the velocities of augmented systems converge to a scaled multiple of each desired velocity field for cooperative mobile robot systems. In this paper, we will focus on how to realize the specification above by decentralized PVFC controller though a centralized PVFC.

2. REVIEW OF PASSIVE VELOCITY FIELD CONTROL (PVFC)

Passive velocity field control (PVFC) had been proposed by Li and the geometry of controlled systems is analyzed (Li, 1999). The methodology encoded tasks using time invariant desired velocity fields instead of the more traditional method. In this section, we briefly review and summarize the design procedure for and properties of an original PVFC.

We consider a n degree of freedom (DOF) fully actuated mechanical system with configuration space subjected to both control forces T and environment forces F_e . Its dynamics can be expressed geometrically in terms of coordinates as follows:

$$M(q)\ddot{q} + C(q, \dot{q})\dot{q} = T + F_e \quad (1)$$

where $M(q)$ and $C(q, \dot{q})$ are the inertia matrix and Coriolis matrix in coordinates, respectively.

The desired velocity field defines a tangent vector at every point of the configuration space, the design methodology will be presented in the following three steps. First, defining an augmented system as a product system with configuration space between plant and a fictitious flywheel system $M_{fw}\ddot{q}_{n+1} = T_{fw}$ as follows:

$$\begin{bmatrix} M(q) & 0 \\ 0 & M_{fw} \end{bmatrix} \begin{bmatrix} \ddot{q} \\ \ddot{q}_{n+1} \end{bmatrix} + \begin{bmatrix} C(q, \dot{q}) & 0 \\ 0 & 0 \end{bmatrix} \begin{bmatrix} \dot{q} \\ \dot{q}_{n+1} \end{bmatrix} = \begin{bmatrix} T \\ T_{fw} \end{bmatrix} + \begin{bmatrix} F_e \\ 0 \end{bmatrix} \quad (2)$$

For the simplicity,

$$M^a(q_a)\ddot{q}_a + C^a(q_a, \dot{q}_a)\dot{q}_a = T^a + F_e^a \quad (3)$$

where $q_a = [q \ q_{n+1}]^T$ is the configuration and M^a is the inertia Riemannian matrix for augmented system. Also, M^a defines the kinetic energy of the augmented system

via:

$$\kappa_a(\dot{q}_a) = \langle\langle \dot{q}_a, \dot{q}_a \rangle\rangle_a := \frac{1}{2} \dot{q}_a^T M^a(q_a) \dot{q}_a \quad (4)$$

where $\langle\langle \cdot, \cdot \rangle\rangle_a$ denotes the inner product defined by the inertia metric M^a . In the following, the system is referred to an augmented system and the terms are suffixed with a . It should be noted that the degree of freedom of Equation (3) is increased from n to $n+1$, and its additional freedom can be considered to be a flywheel which stores and discharges the energy.

Secondly, defining an augmented desired velocity field of the form; $V^a(q_a) = [V(q) \ V^{n+1}(q^{n+1})]^T$, such that the kinetic energy of the augmented system is constant as follows:

$$\kappa_a(V^a) = \frac{1}{2} V_a^T M^a V_a = \bar{E} \quad (5)$$

Therefore a coupling control law T^a in eq. (3) of the form:

$$\begin{aligned} T^a &= \frac{1}{2\bar{E}} (\underbrace{\Delta Q^T - Q\Delta^T}_{=G(q_a, \dot{q}_a)}) \dot{q}_a + \gamma \underbrace{(Qp^T - pQ^T)}_{=R(q_a, \dot{q}_a)} \dot{q} \\ &:= G(q_a, \dot{q}_a) \dot{q}_a + \gamma R(q_a, \dot{q}_a) \dot{q}_a \end{aligned} \quad (6)$$

where $\Delta = M^a \dot{V}_a + C^a V_a$ is the momentum associated with covariant derivative of desired velocity with respect to an actual velocity for system, $p = M^a \dot{q}_a$ and $Q = M^a V_a$ are momentum and desired momentum of an augmented system, respectively. $\gamma \in \mathfrak{R}$ is gain which is a control constant coefficient. Also, $G(q_a, \dot{q}_a)$ and $R(q_a, \dot{q}_a)$ are skew-symmetric matrices and depend on the augmented velocity field $V_a(q_a)$.

To these ends, the formulation of PVFC has two distinct features as follows:

- (1) The task is encoded desired behavior of the mechanical system is specified in terms of velocity field defined on the configuration manifold of the system;
- (2) The mechanical system under closed-loop control appears to be an energetically passive system to its physical environments.

Note that the mechanical system is not required to be at a particular position at each time. Instead, the velocity field guides the robot to approach the contour in a well behaved manner. Moreover, the motivations for developing PVFC were to tackle robotic applications that required; *i) intimate interaction between the machine and uncertain physical environments* and *ii) the coordination between the various DOF of the machine for the task to be accomplished*. The readers are referred to the companion papers (Li, 1999 and 2001) for details.

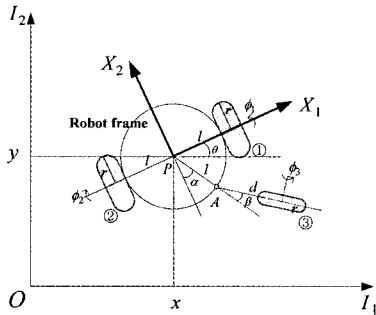


Figure 1. Configuration of a 3-wheeled mobile robot.

3. MULTIPLE 3-WHEELED MOBILE ROBOTS

A wheeled mobile robot (WMR) is a wheeled vehicle which is capable of an autonomous motion without external human driver because it is equipped with motors driven by an embarked computer for its motion such as automated guided vehicle (AGV). We assume that the WMR are made up of a rigid frame equipped with non-deformable wheels and that they are moving on a horizontal plane.

3.1. Description of a 3-Wheeled Mobile Robots

In this section, we consider a 3-wheeled mobile robot with two conventional fixed wheels on the same axle and one conventional off-centered orientable wheel as shown in Figure 1. The two conventional fixed wheels (① and ②) have a fixed orientation while the orientation of wheel ③ is varying.

According to these descriptions, the geometry of the wheels is completely described by the following class; $\{r, l, d, \alpha, \beta, \phi_i; i=1, 2, 3\}$, where the length from the center point P to the center of each wheel is denoted by l , the radius of each wheel is defined by r , and the position of a point A with respect to the trolley is specified by the length l and the angle α . Also, the center of the wheel ③ is connected to the trolley by a rigid rod d (constant) and the rotation angle of this rod is denoted by angle β . The rotation angle of the wheels around their horizontal axis are denoted by $\phi_i (i=1, 2, 3)$. Therefore, the position of the wheel is characterized by a set of four constants $\{r, l, d, \alpha\}$, and its motion by 2 varying angles $\beta(t)$ and $\phi_i(t)$. Moreover if the rod of wheel ③ is fixed, then the angle β becomes obviously a constant (D'Andrea-Novel, 1991).

In Figure 1, we know the vector ξ to indicate the motion of robot body:

$$\xi = (x \ y \ \theta)^T \quad (7)$$

Furthermore, we can introduce the generalized coordinate vector to describe the whole motion of robot as follows:

$$q(t) = (x \ y \ \theta \ \beta \ \phi_1 \ \phi_2 \ \phi_3)^T \quad (8)$$

Using the generalized coordinate vector in Equation (8) and the kinematical constraints by the following constraints; i) pure rolling condition and ii) non-slipping condition, we can also represented the dynamic equation of a 3-wheeled mobile robot by

$$H(\beta) \dot{\zeta}(t) + f(\beta, \zeta) = G(\beta) \tau_m \quad (9)$$

And it is easily shown that these constraints are nonholonomic constraints for the system since two vector fields which satisfy the conditions are not involutive (Compton *et al.*, 1996).

If we assume some conditions and use the following coordinate change

$$\begin{aligned} \zeta_1 &= -\dot{x} \sin \theta + \dot{y} \cos \theta \\ \zeta_2 &= \dot{\theta} \end{aligned} \quad (10)$$

and input transformation, we can obtain the simplified dynamic equation as follows:

$$\begin{pmatrix} \dot{\phi} \\ \dot{\theta} \\ \dot{x} \\ \dot{y} \\ \dot{\beta} \\ \dot{\zeta}_1 \\ \dot{\zeta}_2 \end{pmatrix} \begin{pmatrix} \zeta_1 \\ \zeta_2 \\ -\zeta_1 \sin \theta \\ \zeta_1 \cos \theta \\ -\frac{1}{d} \zeta_1 \sin \beta - \frac{1}{d} \zeta_2 (d + l \cos \beta) \\ v_1 \\ v_2 \end{pmatrix} \quad (11)$$

where $v = (v_1 \ v_2)^T$ is a new input, and the constraints are also represented by (Yamakita, 2000):

$$\begin{aligned} \dot{x} \cos \theta + \dot{y} \sin \theta &= 0 \\ -\dot{x} \sin \theta + \dot{y} \cos \theta &= \zeta_1 \end{aligned} \quad (12)$$

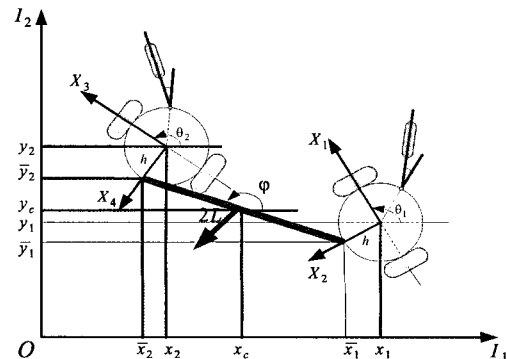


Figure 2. Configuration of cooperative 3-WMRs.

3.2. Cooperative 3-Wheeled Mobile Robots

We consider a case where two WMRs convey a rod for simplicity, however, the similar discussion can be applied for cases where more mobile robots is carrying a general planer rigid object. In this section, we describe the configuration of cooperative 3-WMRs as shown in Figure 2. In considered robot systems, an object denoted by a rod is connected to each mobile robot by a free joint without friction and the length of an object is $2L$.

If we assume that mass and inertia of an object are m and I_o , and a position of the mass center and rotational angle of an object from $O-I_1$ in counterclockwise direction are (x_c, y_c) and φ , then we have free dynamic equations of an object as follows:

$$M_o \ddot{x}_o = 0, \quad I_o \ddot{\varphi} = 0 \quad (13)$$

where

$$M_o = \begin{pmatrix} m & 0 \\ 0 & m \end{pmatrix}, \quad x_o = (x_c \ y_c)^T \quad (14)$$

On the other hand, since the dynamic equation for two 3-WMRs can be described by the previous section, an augmented dynamic equation is represented as follows:

$$H^*(\beta) \dot{\eta}(t) + F^*(\beta, \eta) = G^*(\beta) u(t) \quad (15)$$

where

$$H^* = \begin{pmatrix} H_1(\beta_1) & 0 \\ 0 & H_2(\beta_2) \end{pmatrix}, \quad F^* = \begin{pmatrix} f_1(\beta_1, \eta_1) \\ f_2(\beta_2, \eta_2) \end{pmatrix}$$

$$G^*(\beta) = \begin{pmatrix} G_1(\beta_1) & 0 \\ 0 & G_2(\beta_2) \end{pmatrix}, \quad u(t) = (\tau_{m1} \ \tau_{m2})^T$$

$$\eta_1(t) = (\zeta_1 \ \zeta_2)^T, \quad \eta_2(t) = (\zeta_3 \ \zeta_4)^T,$$

$$\eta(t) := (\eta_1 \ \eta_2)^T$$

Moreover, $\zeta_i \in \mathfrak{R}$, ($i = 1, 2, 3, 4$) is also defined in the previous section, i.e., each subscript number indicates a number of mobile robot except for ζ_i . As ζ_i disappear alone in the following, we note that there should be no confusion.

Using the dynamic equations of an object and each mobile robot, the whole dynamic system without constraint introduced by passive joints can be represented as follows:

$$M_w \ddot{x}_w + F_w = G_w u \quad (16)$$

where

$$M_w = \begin{pmatrix} H^*(\beta) & 0_{1 \times 2} & 0 \\ 0_{1 \times 4} & M_o & 0 \\ 0_{1 \times 4} & 0_{1 \times 2} & I_o \end{pmatrix}, \quad F_w = \begin{pmatrix} F^*(\beta, \eta) \\ 0 \\ 0 \end{pmatrix},$$

$$G_w = (G^* \ 0 \ 0)^T, \quad \dot{x}_w = (\eta_1 \ \eta_2 \ \dot{x}_o \ \dot{\varphi})^T$$

From the kinematic constraints by the passive joints, the holonomic constraints between the generalized coordinates are defined as follows:

$$\begin{pmatrix} \bar{x}_1 \\ \bar{y}_2 \end{pmatrix} = \begin{pmatrix} x_1 - h \sin \theta_1 \\ y_1 + h \cos \theta_1 \end{pmatrix} = \begin{pmatrix} x_c - L \cos \varphi \\ y_c + L \sin \varphi \end{pmatrix} \quad (17)$$

$$\begin{pmatrix} \bar{x}_2 \\ \bar{y}_2 \end{pmatrix} = \begin{pmatrix} x_2 - h \sin \theta_2 \\ y_2 + h \cos \theta_2 \end{pmatrix} = \begin{pmatrix} x_c + L \cos \varphi \\ y_c - L \sin \varphi \end{pmatrix} \quad (18)$$

Then, since these equations can also be rewritten using the differential of Equations (17), (18) and $\eta_i(t)$, ($i = 1, 2$), we can simply represent above equations as matrix form

$$\underbrace{\begin{pmatrix} J_1 & 0_{2 \times 2} & J_o & J_\varphi \\ 0_{2 \times 2} & J_2 & & \end{pmatrix}}_{:=J_w} \begin{pmatrix} \eta_1(t) \\ \eta_2(t) \\ \dot{x}_o \\ \dot{\varphi} \end{pmatrix} = \begin{pmatrix} 0_{2 \times 1} \\ 0_{2 \times 1} \\ 0_{2 \times 1} \\ 0 \end{pmatrix} \quad (19)$$

where

$$J_i = \begin{pmatrix} -\sin \theta_i & -h \cos \theta_i \\ \cos \theta_i & -h \sin \theta_i \end{pmatrix}, \quad J_o = (-I_{2 \times 2} \ -I_{2 \times 2})^T$$

$$J_\varphi = (-L \sin \varphi \ -L \cos \varphi \ L \sin \varphi \ L \cos \varphi)^T$$

Then, the actual dynamic equation for whole systems can be represented as follows:

$$M_w \ddot{x}_w + F_w = G_w u - J_w^T \lambda \quad (20)$$

where λ is a constraint force vector defined by

$$\lambda = (\lambda_1 \ \lambda_2)^T \quad (21)$$

$$\lambda_1 = (\lambda_{m1} \ \lambda_{m2})^T \text{ and } \lambda_2 = (\lambda_{m3} \ \lambda_{m4})^T \quad (22)$$

If we define the constraint force as above equations, the actual dynamic equation of whole system can be decomposed into the following equations using Equation (20)

$$H_i(\beta_i) \dot{\eta}(t) + f_i(\beta_i, \eta_i) = G_i(\beta_i) \tau_{mi} - J_i^T \lambda_i \quad (23)$$

$$M_o \ddot{x}_o = -J_o^T \lambda, \quad I_o \ddot{\varphi} = -J_\varphi^T \lambda \quad (24)$$

3.3. Minor Loop Compensation Scheme

Since we assume that the constraint forces, λ_i ($i = 1, 2$) in Equation (22) are observed by each force sensor in our control method, then we can define a local control input, τ_{mi} ($i = 1, 2$) given by

$$\tau_{mi} = G_i^{-1} (H_i v_i + f_i + J_i^T \lambda_i) - G_i^{-1} H_i J_i^T \lambda_i \quad (25)$$

where v_i ($i = 1, 2$) is new input. If we inject new control input v_i into cooperative mobile robots, then the closed loop system becomes

$$\dot{\eta}_i(t) = v_i(t) - J_i^T \lambda_i \quad (i = 1, 2) \quad (26)$$

Therefore the actual dynamic equation of whole system is represented by

$$\bar{M}_w \ddot{x}_w = \bar{G}_w v(t) - J_w^T \lambda \quad (27)$$

where

$$\bar{M}_w = \begin{pmatrix} I_{2 \times 2} & & & \\ & I_{2 \times 2} & & \\ & & M_o & \\ & & & I_o \end{pmatrix}, \quad \bar{G}_w = \begin{pmatrix} I_{2 \times 2} & 0_{2 \times 2} \\ 0_{2 \times 2} & I_{2 \times 2} \\ & 0_{2 \times 4} \\ 0_{1 \times 4} \end{pmatrix},$$

$$v = (v_1 \ v_2 \ 0 \ 0)^T$$

Note that the minor loop compensation is not necessary for the design of passive velocity field control, however the computation for PVFC would become very complex. Since the dynamic equation is transformed by a coordinate transformation and input change in advance so that the dynamic system of φ disappear in the equation, therefore the control input for φ is realized as an internal force for the motion of x_o .

Let's define $\dot{\bar{x}}_i$ as follows:

$$\dot{\bar{x}}_i = J_i \eta_i(t) \quad (i = 1, 2) \quad (28)$$

Then, using the new coordinate \bar{x}_i , the actual dynamic equation of 3-wheeled mobile robots given by Equation (27) can be rewritten by

$$J_i^{-1} \ddot{\bar{x}}_i - J_i^{-1} \dot{J}_i J_i^{-1} \dot{\bar{x}}_i = v_i - J_i^T \lambda_i \quad (i = 1, 2) \quad (29)$$

Therefore, the actual dynamic equation of whole system can be represented as follows:

$$\begin{pmatrix} J_1^{-1} & & & \\ & J_2^{-1} & & \\ & & M_o & \\ & & & I_o \end{pmatrix} \begin{pmatrix} \ddot{\bar{x}}_1 \\ \ddot{\bar{x}}_2 \\ \ddot{x}_o \\ \ddot{\varphi} \end{pmatrix} + \begin{pmatrix} -J_1^{-1} \dot{J}_1 J_1^{-1} \dot{\bar{x}}_1 \\ -J_2^{-1} \dot{J}_2 J_2^{-1} \dot{\bar{x}}_2 \\ 0_{2 \times 1} \\ 0 \end{pmatrix} = \begin{pmatrix} v_1 \\ v_2 \\ 0_{2 \times 1} \\ 0 \end{pmatrix} - \begin{pmatrix} J_1^T & 0_{2 \times 2} \\ 0_{2 \times 2} & J_2^T \\ J_o^T & \\ J_\varphi^T & \end{pmatrix} \begin{pmatrix} \lambda_{m1} \\ \lambda_{m2} \\ \lambda_{m3} \\ \lambda_{m4} \end{pmatrix} \quad (30)$$

Substituting $\dot{\bar{x}}_i$ defined by Equation (28) into Equation (19) and Defining the matrix \bar{J}_w as follows:

$$\bar{J}_w := \begin{pmatrix} J_1^{-T} & & & \\ & J_2^{-T} & & \\ & & I_{2 \times 2} & \\ & & & 1 \end{pmatrix} \quad (31)$$

Then, pre-multiplying a matrix defined by Equation (31) in Equation (30), we can describe new dynamic equation of whole system as follows:

$$\begin{pmatrix} J_1^{-T} J_1^{-1} & & & \\ & J_2^{-T} J_2^{-1} & & \\ & & M_o & \\ & & & I_o \end{pmatrix} \begin{pmatrix} \ddot{\bar{x}}_1 \\ \ddot{\bar{x}}_2 \\ \ddot{x}_o \\ \ddot{\varphi} \end{pmatrix} + \begin{pmatrix} -J_1^{-T} J_1^{-1} \dot{J}_1 J_1^{-1} \dot{\bar{x}}_1 \\ -J_2^{-T} J_2^{-1} \dot{J}_2 J_2^{-1} \dot{\bar{x}}_2 \\ 0 \\ 0 \end{pmatrix} = \begin{pmatrix} J_1^{-T} v_1 \\ J_2^{-T} v_2 \\ 0 \\ 0 \end{pmatrix} - \underbrace{\begin{pmatrix} I_{2 \times 2} & & & \\ & I_{2 \times 2} & & \\ -I_{2 \times 2} & & -I_{2 \times 2} & \\ & & & J_\varphi \end{pmatrix}}_{:= J_c^T} \begin{pmatrix} \lambda_{m1} \\ \lambda_{m2} \\ \lambda_{m3} \\ \lambda_{m4} \end{pmatrix} \quad (32)$$

Moreover, using the generalized coordinates in Equation (19), J_c^T to Equation (32) is also derived by

$$J_c \dot{\bar{x}}_w = 0 \quad (33)$$

where

$$\bar{x}_w = (\bar{x}_1 \ \bar{x}_2 \ x_o \ \varphi)^T \quad (34)$$

Furthermore if we define new input $v_i(t)$ in Equation (25) as

$$v_i(t) = J_i^{-1} (v_i - \dot{J}_i J_i^{-1} \dot{\bar{x}}_i) + (J_i^T - J_i^{-1}) \lambda_i \quad (35)$$

Then the whole dynamic equations using Equation (32) and new coordinate x_i ($i = 1, 2$) can be represented as follows:

$$\bar{M}_w \ddot{\bar{x}}_w = (v_1 \ v_2 \ 0_{2 \times 1} \ 0)^T - J_c^T \lambda \quad (36)$$

$$J_c \dot{\bar{x}}_w = 0 \quad (37)$$

where v_i ($i = 1, 2$) is an actual control input.

Using the generalized coordinate and the differentiation given by Equations (17), (18), we can derive the following equations from the relationship between the position of mass center $x_o = (x_c \ y_c)^T$ and new coordinate \bar{x}_i ($i = 1, 2$) as follows:

$$\begin{pmatrix} \dot{x}_c \\ \dot{y}_c \end{pmatrix} = \underbrace{\begin{pmatrix} -\sin \theta_1 & -h \cos \theta_1 \\ \cos \theta_1 & -h \sin \theta_1 \end{pmatrix}}_{:= J_1 \eta_1 = \dot{\bar{x}}_1} \begin{pmatrix} \zeta_1 \\ \zeta_2 \end{pmatrix} + \underbrace{\begin{pmatrix} -L \sin \varphi \\ -L \cos \varphi \end{pmatrix}}_{:= (I_{2 \times 2} \ 0_{2 \times 2}) J_\varphi} \dot{\varphi} \quad (38)$$

$$\begin{pmatrix} \dot{x}_c \\ \dot{y}_c \end{pmatrix} = \underbrace{\begin{pmatrix} -\sin \theta_2 & -h \cos \theta_2 \\ \cos \theta_2 & -h \sin \theta_2 \end{pmatrix}}_{:= J_2 \eta_2 = \dot{\bar{x}}_2} \begin{pmatrix} \zeta_3 \\ \zeta_4 \end{pmatrix} + \underbrace{\begin{pmatrix} L \sin \varphi \\ L \cos \varphi \end{pmatrix}}_{:= (0_{2 \times 2} \ I_{2 \times 2}) J_\varphi} \dot{\varphi} \quad (39)$$

for simplicity,

$$\dot{x}_o = \dot{\bar{x}}_1 + (I_{2 \times 2} \ 0_{2 \times 2}) J_\varphi \dot{\varphi} \quad (40)$$

$$\dot{x}_o = \dot{\bar{x}}_2 + (0_{2 \times 2} \ I_{2 \times 2}) J_\varphi \dot{\varphi} \quad (41)$$

Furthermore, substituting the differentiations of Equations (40), (41) into Equation (36), we can also describe as follows:

$$\ddot{\bar{x}}_o - (I_{2 \times 2} \quad 0_{2 \times 2})(J_\varphi \ddot{\varphi} + \dot{J}_\varphi \dot{\varphi}) = v_1 - \lambda_1 \quad (42)$$

$$\ddot{\bar{x}}_o - (0_{2 \times 2} \quad I_{2 \times 2})(J_\varphi \ddot{\varphi} + \dot{J}_\varphi \dot{\varphi}) = v_2 - \lambda_2 \quad (43)$$

4. VIRTUAL PASSIVITY-BASED DECENTRALIZED CONTROL ALGORITHM

In order to design the decentralized PVFC, we assume that $\ddot{\varphi}$ is measurable for each subsystem in this paper. Since $\ddot{\varphi}$ is determined based on both λ_1 and λ_2 , and both signals can not be used for each subsystem in the decentralized formulation. The proposed scheme in this paper is shown in Figure 3.

If the actual control input is defined as

$$v_1 = v_1' - (I_{2 \times 2} \quad 0_{2 \times 2})(J_\varphi \ddot{\varphi} + \dot{J}_\varphi \dot{\varphi}) \quad (44)$$

$$v_2 = v_2' - (0_{2 \times 2} \quad I_{2 \times 2})(J_\varphi \ddot{\varphi} + \dot{J}_\varphi \dot{\varphi}) \quad (45)$$

Adding the dynamic equation of \bar{x}_o , we can describe the motion equation of an object as follows:

$$(I_{2 \times 2} + M_o + I_{2 \times 2})\ddot{\bar{x}}_o = v_1' + v_2' \quad (46)$$

First of all, the procedure in order to apply an individual PVFC algorithm can be designed that the motion equation in Equation (46) is separated as the following virtual dynamic equation

$$(I_{2 \times 2} + \rho_1 M_o)\ddot{\bar{x}}_o = v_1' \quad (47)$$

$$(I_{2 \times 2} + \rho_2 M_o)\ddot{\bar{x}}_o = v_2' \quad (48)$$

for simplicity,

$$\bar{M}_i' \ddot{\bar{x}}_o = v_i' \quad (i = 1, 2) \quad (49)$$

where $\rho_i (i = 1, 2)$ is load sharing coefficient and it is satisfied with $\rho_1 + \rho_2 = 1$.

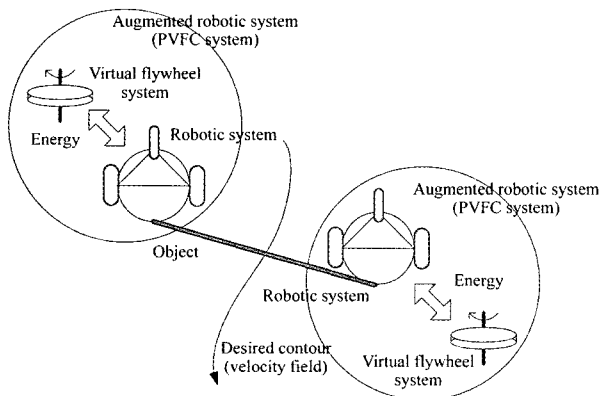


Figure 3. Conception of decentralized PVFC scheme.

Also, the dynamics of the virtual flywheel is given by

$$M_{fwi} \ddot{x}_{fwi} = v_{fwi} \quad (i = 1, 2) \quad (50)$$

where v_{fwi} is the coupling control input to the flywheel. Thus, the dynamics of the augmented system are composed as follows:

$$\bar{M}_{ai}' \ddot{\bar{x}}_o = v_i' \quad (i = 1, 2) \quad (51)$$

where $\dot{X}_{ai} = (\dot{\bar{x}}_o \quad \dot{x}_{fwi})^T$ is the velocity of the augmented system, v_{ai}' is the augmented control input, and M_{ai}' is the augmented inertia matrix and is defined by

$$\bar{M}_{ai}' = \begin{pmatrix} \bar{M}_i' & 0 \\ 0 & M_{fwi} \end{pmatrix} \quad (52)$$

For each augmented configuration X_{ai} , we can define the kinetic energy of the augmented dynamic system, \bar{H}_a' which is expressed in local coordinate by

$$\bar{H}_a' = \sum_{i=1}^2 \frac{1}{2} \dot{X}_{ai}^T \bar{M}_{ai}' \dot{X}_{ai} \quad (53)$$

For the augmented mechanical system, an augmented desired velocity field V_{ai} is needed and it is defined by section 2.

Condition 1: The augmented desired velocity field satisfies:

Conservation of kinetic energy: The total kinetic energy of the augmented system evaluated at the desired velocity field is constant.

$$\bar{H}_a' = \sum_{i=1}^2 \frac{1}{2} \dot{X}_{ai}^T \bar{M}_{ai}' \dot{X}_{ai} = \bar{E}_i > 0 \quad (54)$$

where \bar{E}_i is a positive constant.

Consistency: The component of the augmented velocity field that corresponds to the original dynamic equation of motion system should be the same as the specified desired velocity field.

$$V_{ai} = (V_i \quad V_{n+1})^T \quad (55)$$

Notice that $\bar{E}_i (i = 1, 2)$ should be selected to be large enough so that Equation (54) has a real solution. It should now be apparent that the virtual inertia acts as a reservoir of kinetic energy.

Then the coupling control law is given by (Yamakita *et al.*, 2000)

$$\dot{v}_{ai}' = (\bar{G}_{ai} + \gamma_i \bar{R}_{ai}) X_{ai} \quad (i = 1, 2) \quad (56)$$

where

$$\bar{G}_{ai}(X_{ai}, \dot{X}_{ai}) = \frac{1}{2\bar{E}_i} \underbrace{(\bar{\Delta}_{ai} \bar{Q}_{ai}^T - \bar{Q}_{ai} \bar{\Delta}_{ai}')}_{\text{skew symmetric}} \quad (57)$$

$$\bar{R}_{ai} = \underbrace{\bar{Q}_{ai}\bar{P}_{ai}^T - \bar{P}_{ai}\bar{Q}_{ai}^T}_{\text{skew symmetric}} \quad (58)$$

and $\gamma(i=1, 2)$ is a control gain, not necessary positive. For any $\alpha_i \in \mathfrak{R}$, the local coordinate representation of the augmented α_i -velocity error e_{ai} is defined by

$$e_{ai} = \dot{X}_{ai} - \alpha_i V_{ai} \quad (59)$$

Thus, we can obtain the error dynamics for the augmented system in Equation (50) as follows:

$$\bar{M}_{ai}' \dot{e}_{ai} = \bar{G}_{ai} e_{ai} + \gamma_i \bar{R}_{ai} \dot{X}_{ai} \quad (60)$$

Theorem 1: Consider the decentralized PVFC as shown in Figure 3 where the motion equation is given by Equation (49), and the individual PVFC control law consists of the virtual dynamic augmentation Equation (50) and coupling control law Equation (56). Furthermore if the control input about control internal force is defined by

$$v_{i1}' = (1 + k_f) \begin{pmatrix} F_{di} \\ 0 \end{pmatrix} \quad (61)$$

and an actual control input about given system v_i' is also defined by

$$v_i' = v_{ai}' + v_{i1}' \quad (i=1, 2) \quad (62)$$

where v_{i1}' is desired internal force and satisfies $v_{i1}' + v_{i2}' = 0$. Then the passivity and convergence properties of decentralized PVFC are summarized as follows:

(1) The augmented feedback system is passive with respect to the supply rate defined by

$$s(F, \dot{x}) = \langle F, \dot{x} \rangle = F^T \dot{x} \quad (63)$$

where and are input and output.

(2) For the augmented α_i -velocity error e_{ai} , the velocity of an object \dot{X}_{ai} is a Lyapunov stable solution in the absence of environment forces.

See Appendix for proofs. ■

Furthermore the constraint force λ_i converges to

$$\beta \rho_i M_o \frac{\partial V}{\partial x_o} V + v_{i1}' \quad (64)$$

where β is a scalar number and V is a desired velocity field. So if we set

$$\begin{pmatrix} v_{i1}' \\ v_{i2}' \end{pmatrix} := v_i' = \frac{J_\varphi}{\|J_\varphi\|^2} v_\varphi + J_\varphi^* v_l \quad (65)$$

where v_φ is a control input for φ and v_l is control for an internal force which does not affect the linear nor angular motion of an object, and

$$J_\varphi^* = (\cos \varphi \quad -\sin \varphi \quad -\cos \varphi \quad \sin \varphi)^T \quad (66)$$

So we can control the linear motion of an object by individual PVFC and both φ and λ_i can also be controlled to desired values.

5. SIMULATION RESULTS

This section illustrates the performance of the proposed control algorithm for cooperative 3-WMRs using numerical simulations. The considered dynamic models will use the similar ones for experiment and is shown in Figure 4 based on the constructed experimental system.

5.1. Simulation conditions

In Equations (41), (42), they conclude $\ddot{\varphi}$ which actually is impossible to measure. Therefore, we need to use the estimate value of $\ddot{\varphi}$. Assume that $\varphi^{(3)} = 0$, we compose an observer about the following state equation

$$\begin{pmatrix} \dot{\varphi} \\ \ddot{\varphi} \\ \varphi^{(3)} \end{pmatrix} = \begin{pmatrix} 0 & 1 & 0 \\ 0 & 0 & 1 \\ 0 & 0 & 0 \end{pmatrix} \begin{pmatrix} \varphi \\ \dot{\varphi} \\ \ddot{\varphi} \end{pmatrix} \quad (67)$$

The observer can be represented by *Gopinath's design method* as follows:

$$\dot{\zeta} = -K_{ob} \zeta - K_{ob}^2 \dot{\varphi} \quad (68)$$

$$\hat{\ddot{\varphi}} = \zeta + K_{ob} \dot{\varphi}$$

where K_{ob} is observer gain.

Since the desired velocity field is defined such that if a point moves along the desired velocity, the point converges to a circle whose center and radius are the origin and 1[m] at a constant speed in a anti-clockwise direction. For the control of angle of an object φ , desired angle and angular velocity φ_d and $\dot{\varphi}_d$ are defined as follows:

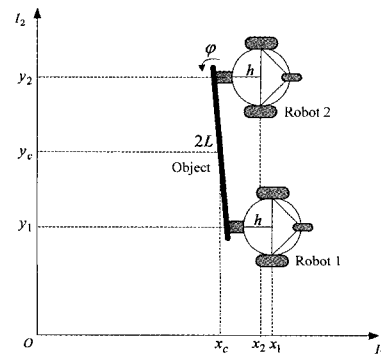


Figure 4. Configuration of cooperative 3-WMR.

Table 1. System parameters and initial states for cooperative mobile robots.

L	0.2 [m]	γ	1.0
\bar{E}_i	5000 [Nm]	M_{fwi}	1.0
x_{fwi}	0.0	\dot{x}_{fwi}	10.0
K_v	4.0	K_p	4.0
(x_1, y_1)	(1,1)	(x_2, y_2)	(1,1)
θ_1	$\pi/2$	θ_2	$\pi/2$
β_i	0.0	φ	-1.7

$$\varphi_d = -\tan^{-1}\left(\frac{y_c}{x_c}\right), \quad \dot{\varphi}_d = \frac{d}{dt}\varphi_d \Big|_{\substack{\dot{x}_c = \dot{x}_{cd} \\ \dot{y}_c = \dot{y}_{cd}}} \quad (69)$$

where \dot{x}_{cd} and \dot{y}_{cd} are the desired velocity specified by a desired velocity field in decentralized PVFC as shown in Figure 4, respectively.

A control input is determined by

$$v_\varphi = -K_v(\varphi_d - \varphi) - K_p(\dot{\varphi}_d - \dot{\varphi}) \quad (70)$$

and v_l was set to 0. The control is used for both robots and load sharing parameters ρ_i is set to 0.5 since we assumed that each mobile robot has the same capability. For the observation of $\tilde{\varphi}$, we will use a minimal order observation which is designed based on triple integrator model where the pole of the observer was chosen to -50 . The various system parameters and the initial states used in numerical simulations are shown in Table 1.

5.2. Simulation Results

When we are include the external force (10,0)[N] to system from $t = 15[\text{sec}]$ to $t = 20[\text{sec}]$, the simulation results for considered system are shown in Figures 5–9, respectively.

The desired trajectories and actual trajectories for cooperative mobile robots and an object are shown in Figure 5, respectively. In this figure, it can be seen that

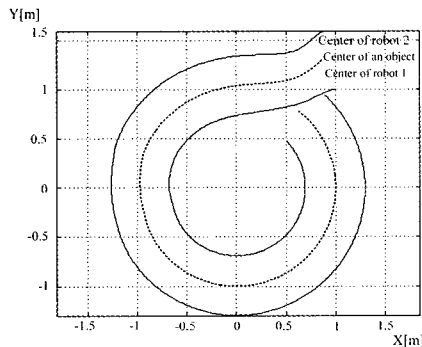


Figure 5. Trajectories for cooperative 3-wheeled mobile robots and an object.

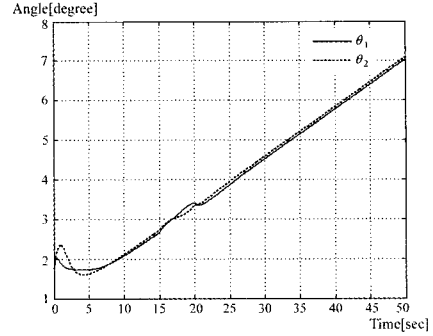


Figure 6. Angle variations of mobile robots.

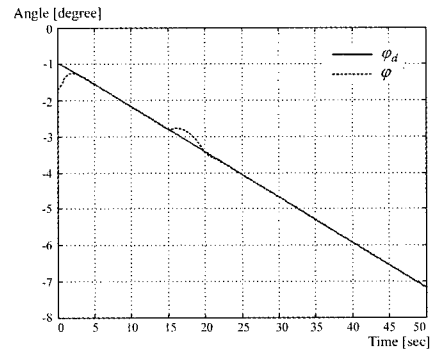


Figure 7. Tracking angle of an angle and desired angle of an object.

the center of an object follows the desired trajectory through some tracking error exists due to uncertainties of parameters and effects of the dead reckoning.

The angle variation of an object is shown in Figure 6, and the tracking performance of angles for the desired signals are shown in Figure 7. It also shows good tracking performance. The constraint force with disturbance is shown in Figure 8. Finally, the changes of virtual energy are plotted in Figure 9. It is seen from the figure that each virtual energy decreases slightly due to energy loss caused by incomplete cancellation of friction effects.

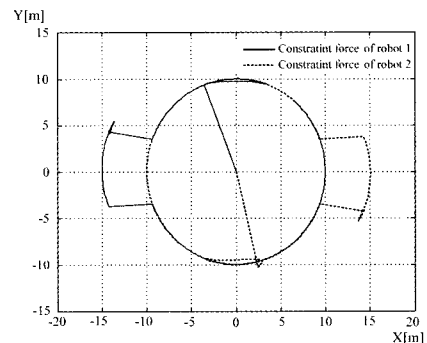


Figure 8. Constraint forces with disturbance.

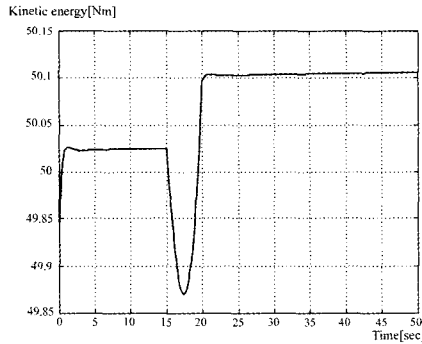


Figure 9. Kinetic energy of augmented system.

6. CONCLUSIONS

In this paper, we propose a new control methodology for cooperative 3-wheeled mobile robotic systems convey a rigid object, and the proposed decentralized control algorithm is also analyzed using PVFC algorithm. Especially, the closed-loop input/output systems for multiple robotic systems are passive with the environment force as inputs, the system velocities as outputs, and the environment mechanical powers as supply rates as if it is similar to an original PVFC. The closed-loop systems for cooperative mobile robots are very effective in tracking a multiple of each desired velocity field and in counteracting the detrimental effect of environment disturbances when the disturbances are in the directions of the desired momentums of multiple robotic systems. Also, the performance will improve when the multiple robot systems are moving at high speed.

ACKNOWLEDGEMENT—The work was supported by the National Research Laboratory Program of the Korean Ministry of Science and Technology (MOST).

REFERENCES

- Campion, G., Bastin, G. and D'Andrea-Novet, B. (1996). Structural properties and classification of kinematic and dynamic models of wheeled mobile robots. *IEEE Trans. on Robotics and Automation* **12**, **1**, 47–62.
- Li, P. Y. and Horowitz, R. (1999). Passive velocity field control of mechanical manipulator. *IEEE Trans. on Robotics and Automation* **15**, **4**, 751–763.
- Li, P. Y. and Horowitz, R. (2001). Passive velocity field control (PVFC) Part I—Geometry and Robustness. *IEEE Trans. on Automatic Control* **46**, **9**, 1346–1359.
- Nouillant, C., Assadian, F., Moreau, X. and Oustaloup, A. (2002). A cooperative control for car suspension and brake systems, *Int. J. Automotive Technology* **3**, **4**,

147–155.

- Slotine, J. J. and Li, W. (1991). *Applied Nonlinear Control*. Prentice-Hall, New Jersey.
- Suh, J. H., Yamakita, M. and Kim, S. B. (2004). Adaptive desired velocity field control for cooperative mobile robotic systems with decentralized PVFC. *The Japan Society of Mechanical Engineers (JSME) Int. J. Series-C* **47**, **1**, 280–288.
- Suh, J. H. and Lee, K. S. (2004). Decentralized control of cooperative mobile robot systems using passive velocity field control method. *Trans. Korean Society of Automotive Engineers* **12**, **4**, 129–138.
- Yamakita, M., Suzuki, K., Zheng, X. and Ito, K. (1998). Cooperative control for multiple manipulator using an extended passive velocity field control, *Trans. on IEE Japan*, **180-C**, **1**, 21–28.
- Yamakita, M., Suh, J. H. and Hashiba, K. (2000). Decentralized PVFC for cooperative mobile robots, *Trans. on IEE Japan* **120-C**, **10**, 1485–1491.

APPENDIX

Proof of (1) in Theorem 1: The derivation of kinetic energy defined by Equation (54) satisfies

$$\begin{aligned}
 \frac{d}{dt} \bar{H}'_{ai} &= \sum_{i=1}^2 (\dot{X}'_{ai} \bar{M}'_{ai} \ddot{X}_{ai} + \frac{1}{2} \dot{X}'_{ai} \bar{M}'_{ai} \dot{X}_{ai}) \\
 &= \sum_{i=1}^2 (\dot{x}'_o \bar{M}'_i \ddot{x}_o + \dot{x}_{fwi} \underbrace{M_{fwi} \ddot{x}_{fwi}}_{=v_{fwi}}) + \frac{1}{2} \sum_{i=1}^2 \dot{X}'_{ai} \bar{M}'_{ai} \dot{X}_{ai} \\
 &= \dot{x}'_o \sum_{i=1}^2 v'_i + \sum_{i=1}^2 \dot{x}_{fwi} v_{fwi} \\
 &= \sum_{i=1}^2 \dot{X}'_{ai} \bar{G}'_{ai} \dot{X}_{ai} + \dot{X}'_{ai} \bar{R}'_{ai} \dot{X}_{ai} \\
 &= 0
 \end{aligned} \tag{a1}$$

Therefore, upon integration of equation (a1), we can obtain

$$\int_0^t \dot{\bar{H}}'_a(t) dt = \bar{H}'_a(t) - \bar{H}'_a(0) = 0 > -\bar{H}'_a(0) \tag{a2}$$

Since $\bar{H}'_a(0) \geq 0$, the system is passive with respect to the supply rate.

Proof of (2) in Theorem 1: Given $\alpha \in \mathfrak{R}$, let's define the positive definite storage function \bar{W}_α as follows:

$$\bar{W}_\alpha = \frac{1}{2} \sum_{i=1}^2 e^{\alpha t} \bar{M}'_{ai} e_{ai} \tag{a3}$$

Differentiating equation (a3) and the fact that $\bar{M}'_{ai} + 2\bar{G}'_{ai}$ is skew symmetric, we obtain

$$\begin{aligned}
\frac{d}{dt} \bar{W}_\alpha &= \frac{1}{2} \sum_{i=1}^2 (\dot{e}_{ai}^T \bar{M}'_{ai} e_{ai} + \underbrace{e_{ai}^T \bar{M}'_{ai} \dot{e}_{ai}}_{=0} + e_{ai}^T \bar{M}'_{ai} \dot{e}_{ai}) \\
&= - \sum_{i=1}^2 \alpha_i \gamma_i \{ \underbrace{V_{ai}^T \bar{M}'_{ai} V_{ai}}_{=2\bar{E}_i} \cdot \underbrace{\dot{X}_{ai}^T \bar{M}'_{ai} \dot{X}_{ai}}_{=2\bar{H}_{ai}} - \underbrace{(V_{ai}^T \bar{M}'_{ai} \dot{X}_{ai})^2}_{= \langle\langle V_{ai}, \dot{X}_{ai} \rangle\rangle_{ai}^2} \} \quad (\text{a4}) \\
&= - \sum_{i=1}^2 \alpha_i \gamma_i (4\bar{H}'_{ai} \bar{E}_i - \langle\langle V_{ai}, \dot{X}_{ai} \rangle\rangle_{ai}^2) \\
&\leq 0
\end{aligned}$$

Since \bar{W}_α is a positive definite function of α_i -velocity error e_{ai} , we know that the augmented α_i -velocity error $e_{ai}=0$ is *Lyapunove stable* of the error dynamics using Barlalet's lemma (Slotine *et al.*, 1991). ■